J Mol Model (2012) 18:3283–3289
DOI 10.1007/s00894-012-1351-1

ORIGINAL PAPER

Vector correlations in the F + HO → HF + O reaction and its isotopic variant

Dan Zhao · TianShu Chu · Ce Hao

Received: 11 August 2011 / Accepted: 1 January 2012 / Published online: 18 January 2012

Abstract The F + H(D)O → HF(DF) + O reactions have been studied using quasi-classical trajectory (QCT) calculation method, based on the three different potential energy surfaces (PESs) of Gomez-Carrasco et al. (J Chem Phys 2004, 121:4605; J Chem Phys 2005, 123:114310; Chem Phys Lett 2007, 435:188). Facilitated with the analysis of the QCT results, the pictures for product scattering and product polarizations have been presented to investigate the vector correlations in the two reactions, with effects of isotope substitution and electronic state as well as collision energy being revealed at a chemical stereodynamical level.

Keywords Isotopic effect · Quasi-classical trajectory · Stereodynamics · Vector correlations

D. Zhao · C. Hao
School of Chemical Engineering,
Dalian University of Technology,
Dalian 116023, China

D. Zhao · T. Chu
State Key Laboratory of Molecular Reaction Dynamics,
Dalian Institute of Chemical Physics
Chinese Academy of Sciences,
Dalian 116023, China

T. Chu (✉)
Institute for Computational Sciences and Engineering,
Laboratory of New Fiber Materials and Modern Textile,
the Growing Base for State Key Laboratory,
Qingdao University,
Qingdao 266071, China
e-mail: tschu008@163.com

T. Chu
e-mail: tschu@dicp.ac.cn

Introduction

The HOF system is one of the most elementary triatomic systems and can be considered as a model system for HOX (X = F, Cl, Br, etc.). As a consecutive reaction of F + H_2O, the F + HO reaction has attracted much attention. In the past years, researchers endeavored to discover the kinetic and dynamic properties of the HOF system. Due to the corrosive property of HF, experimental data about the H + FO → HF + O reaction is not abundant. Sloan's group implemented experimental work and performed relevant calculations reproducing their measured vibrational distribution [1]. Walther and Wagner have carried out kinetic experiment studying the temperature effect on the rate constants [2]. As is well known, the potential energy surfaces are indispensable to most of kinetics and dynamics theoretical research, such as the WP (wave packet) and most QCT (quasi-classical trajectory) calculations. In 2000, Kornweitz et al. have reported the three-center semi-empirical potential energy surfaces of the F + HX and F + OH reactions [3]. Gómez-Carrasco et al. also investigated the potential surfaces for this OHF reactive system, and they successfully constructed a series of PESs (potential energy surfaces) for the different electronic states of the system [4–6]. Based on these PESs and employed the one for the ^{3}A" electronic state, Gonzalez-Sanchez et al. [7], Zhao et al. [8, 9], and Han et al. [10] reported the stereodynamics characters of the OHF system. With another ^{3}A' state, we investigated the stereodynamics of the two product channels in the H + FO reaction [11]. One of the authors also employed a combined quantum mechanics (QM) and QCT method to explore the H + FO reaction and its isotope variant on the three PESs of the ^{1}A', ^{3}A' and ^{3}A" states [12].

Up to present, there are a great number of theoretical studies for the OHF system. However, an extensive and thorough stereodynamical investigation has not been conducted

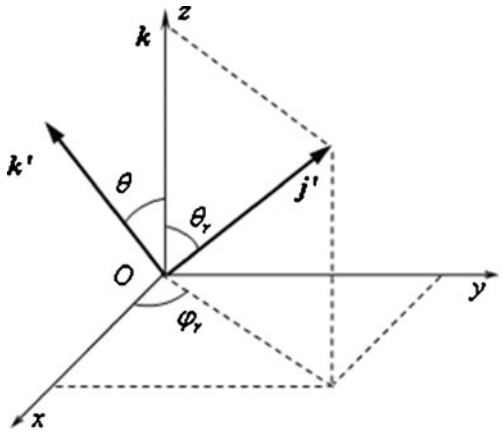

Fig. 1 The center of mass frame describing the ***k***, ***k'*** and ***j'*** correlations

for the F + HO reaction occurring on all of the above-mentioned electronic states. It is this fact which lies behind our present desire to perform a computational study of F + HO (v=0, j=0) → HF + O and its isotopic variant by running trajectories on the three ^{1}A', ^{3}A' and ^{3}A" electronic states. For elucidating the stereodynamics of a chemical reaction, QCT is proved to be one of the most popular methods. The QCT code capable of exploring vector properties in a chemical reactive system from Han's group, as well as those from other research groups [13–16], has been widely employed for the study of chemical reactions [17–28]. Both the scalar and vector properties, including product rovibrational distribution, translational distribution, angular distribution, PDDCS (polarization dependant differential cross section), product alignment and orientation parameters can be produced from the corresponding QCT calculations.

The specific calculation method we employed can be consulted from the references [11, 12, 29–34]. According to the different characters of the three PESs, collision energy in this work is chosen to be in the range from 0.5 eV to 1.0 eV with the interval of 0.1 eV and is referred to that in the center-of-mass (CM) frame used in the present QCT calculation. The initial distance between the fluorine atom and the center of mass of HO is 20 angstrom. The calculations for F + H(D)O have been carried out by running 100,000 trajectories with a time step size of 1 fs. It should be noted that in our QCT calculations, we neglected the spin-orbit coupling in the fluorine atom and thus the electronic angular momentum of the fluorine atom even though it can couple to rotational angular momentum.

Results and discussion

The picture describing vector correlations during the F + HO reaction has been given in Fig. 1. In the figure, ***k*** and ***k'*** represent the reagent and the product relative velocities, ***j'*** denotes the product angular momentum. The correlations among these vectors can be determined with the density probability as a function of the scattering angle θ_t or as a function of the polar angles of θ_r and/or φ_r.

Figure 2 presents the polarization-dependent differential cross section ($PDDCS_{00}$) as a function of both collision energy and scattering angle for F + HO → HF + O, showing the discrepancies in the scattering directions of the products on the three different PESs. The HF products prefer forward scattering on the ^{1}A' and ^{3}A" PESs, whereas they prefer backward scattering on the ^{3}A' PES. The degree of the product scattering on the ^{1}A' state is much greater than that on the two triplet states. With the collision energy increasing, such preference tendency is increasing on the singlet electronic state while decreasing on the ^{3}A' and ^{3}A" states. Figure 3 shows the product scattering in the F + DO → FD + O isotope reaction. Compared with the HF product, the FD product on the ^{1}A' PES exhibits a trend for a forward-backward symmetry, which is caused by the heavy isotope mass; the scattering of the FD product on the ^{3}A" PES has changed to the backward direction; but there is no remarkable differences between the two isotope reactions on the ^{3}A' PES.

It is well known that $(2\pi/\sigma)(d\sigma_{00}/d\omega_t)$ (=$PDDCS_{00}$) describes only the ***k-k'*** correlation or the scattering direction of the products and it is not associated with the orientation and alignment of the product rotational angular momentum vector [35]. In order to further provide insight into the reactions, we calculated the distributions of $P(\theta_r)$ and $P(\varphi_r)$ to elucidate the polarization behaviors of the products. The distributions of $P(\theta_r)$ describing the ***j'-k*** correlation in F + HO → HF + O are shown in Fig. 4. On all three electronic states, the $P(\theta_r)$ distributions peaked at 90 degree which indicated that the product rotational angular momentum is aligned along the

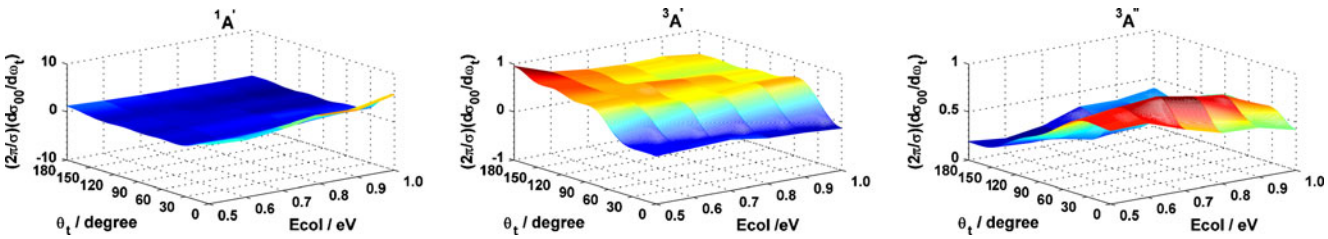

Fig. 2 The QCT differential cross sections $(2\pi/\sigma)(d\sigma_{00}/d\omega_t)$ of F + HO → HF + O as a function of scattering angle and collision energy ranging from 0.5 eV to 1.0 eV

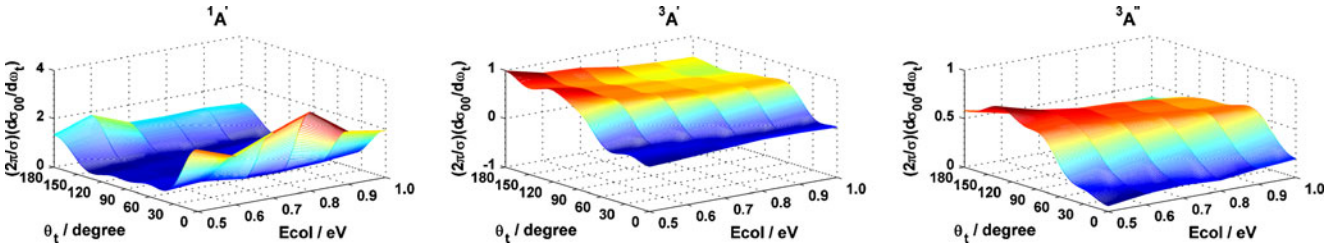

Fig. 3 Similar to Fig.2, but for the reaction of F + DO → DF + O and the collision energy range is the same as Fig.2

direction perpendicular to the reagent relative velocity direction. From the peak height of these distributions on the three states, one can easily find that the strongest product alignment on the singlet state appeared at the collision energy of 0.6 eV, and there is an increasing-then-decreasing trend of the product alignment over the collision energy range on this state; the alignment dependence on collision energy is the weakest on the ^{3}A' state. With respect to the ^{3}A" state, the degree of the product alignment is first decreasing then increasing when collision energies are lower/higher than 0.7 eV. Thus, here the influence of potential energy surfaces on the product alignment and its energy-dependent behavior was really rather remarkable.

Isotope effects on the $P(\theta_r)$ distributions can be examined and shown by comparing Fig. 4 with Fig. 5 where the corresponding results for the isotope variant are presented. Clearly, the product alignment on the singlet state has been weakened largely with isotope substitution, because the $P(\theta_r)$ distributions in Fig. 5 tend to be more isotropic with more oscillations. On the ^{3}A' state, isotope substitution affects more the degree of the product alignment but has little influence on its energy-dependent behavior. For the ^{3}A" state, it is found that with isotope substitution, degree of product alignment shows an increasing tendency with increasing collision energy, which is quite different from the observation in the F + HO reaction. Thus, the comparison showed that influence on the ***k-j'*** correlation of the isotopic effects is relatively significant for the singlet state.

The distributions of $P(\varphi_r)$ that describe the ***k-k'-j'*** correlation are shown in Fig. 6 and Fig. 7 for the two reactions of F + HO and F + DO, respectively. Seen first from Fig. 6, for all electronic states, the appearances of the peaks at 90 degree and at 270 degree verified that the product rotational angular momentum vectors aligned along the y-axis. The F + HO reaction also showed product orientation pointing to the negative direction of the y axis, because of the asymmetric property of the two obvious peaks located at 270 and 90 degrees. Moreover, influences of the collision energy on the product polarization are quite different for the three electronic states: product polarization, that is, product alignment along the y-axis and product orientation to the negative direction of y-axis, is found to be reinforced first on the ^{1}A' state with increasing collision energy, reaching the maximum at the collision energy of 0.8 eV, then it decreased to some extent with the continued increasing of the collision energy. Contrary to this, there is an overall decreasing trend of the polarization degree on both triplet states, with that on the ^{3}A" state illustrating more sensitivity to the collision energy.

Influence of isotope substitution on the above-mentioned product alignment and orientation can be provided by analyzing the two figures of Fig. 6 and Fig. 7. We see that isotope effects do affect the product polarization, causing more oscillations in the $P(\varphi_r)$ distributions on the ground singlet state. This phenomenon indicates a tendency for the product isotropy in the heavy isotope variant, similarly to that seen in the $P(\theta_r)$ distribution on the same electronic state. Moreover, due to isotope substitution the product polarization is weakened on both triplet states. However, the energy-dependent behavior of product polarization for each of the three electronic states shown in Fig. 7 is quite similar to that in Fig. 6, revealing an insensitivity of this behavior to the isotope effects. As consequence, the isotope

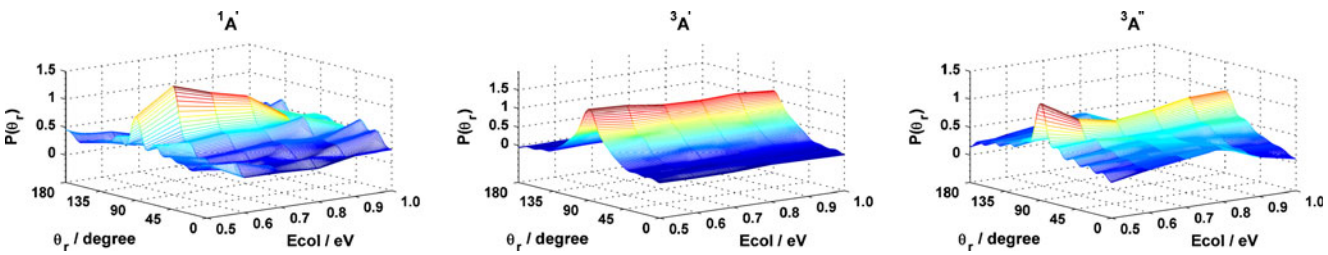

Fig. 4 The distributions of $P(\theta_r)$ reflecting ***k-j'*** correlation for F + HO → HF + O for the collision energies from 0.5 eV to 1.0 eV. The distributions are illustrated as a function of both θ_r and collision energy

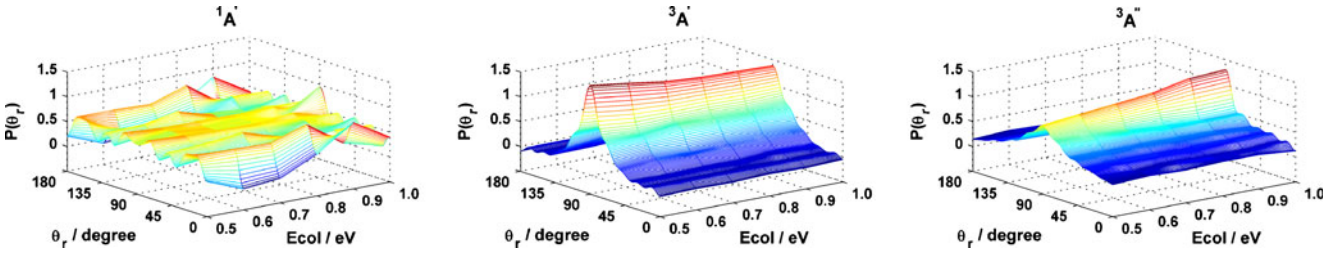

Fig. 5 The distributions of $P(\theta_r)$ reflecting ***k-j'*** correlation for F + DO → DF + O for the collision energies from 0.5 eV to 1.0 eV. The distributions are illustrated as a function of both θ_r and collision energy

substitution can also influence the distributions of the product rotational angular momentum as a function of the azimuthal angle φ_r.

The 3D polar plots of the $P(\theta_r, \varphi_r)$ distributions on the three electronic states are presented for the F + HO reaction in Figs. 8, 9, 10. These jointed distributions are in good accordance with the above discussion concerning the alignment and orientation of the product rotational angular momentum vectors on the three electronic states.

As of now, we have established that the products behaved differently on the three electronic states which can be explained in terms of the different potential energy surface structures shown in Fig. 11. As seen, the ^{1}A' potential energy surface has the deepest well among the three surfaces. This presence of the deepest well will deteriorate the memory of the nascent molecule profile, leading to the observation of a rather weak product polarization on this singlet state. The ^{3}A" state exhibits two rather deep hydrogen-bonded wells, while the ^{3}A' surface presents only a rather shallow well in the reactant channel. Besides, the ^{3}A" surface has lower energy barrier than the ^{3}A' surface. Because of that, product polarization on the ^{3}A' state slightly changes with collision energy in our investigated range, while on the ^{3}A" surface, high collision energy do have effects on the product polarization behaviors. Thus, this further confirmed that the alignment and orientation of the products rely on the topographic features of the potential energy surfaces.

Conclusions

In this work, the stereodynamics of the F + H(D)O reactions are investigated in the collision energy range of 0.5-1.0 eV with the QCT method. The calculation results provided the details of the scattering direction and the way of polarization of the products on the three electronic states of ^{1}A', ^{3}A' and ^{3}A". For the two states of ^{1}A' and ^{3}A", the HF products prefer forward scattering. While on the ^{3}A' state the HF products are backward scattered. However, the DF products on the singlet state are both backward and forward scattered, and those on the ^{3}A" state are scattered in a backward direction while the products on the ^{3}A' state still have the backward scattering. Almost all the products on the three electronic states, in particular the two triplet states, have exhibited strong product alignment perpendicular to ***k*** or along the direction of the y-axis and product orientation pointing to the negative y-axis. For the F + HO reaction, the tendency with collision energy of the product alignment perpendicular to ***k*** is quite different for the singlet and triplet states, namely there is an increasing-then-decreasing trend on the singlet state but a decreasing-then-increasing one on the two triplet states. The product alignment along the y-axis and the product orientation to the negative direction of the y-axis are also affected by collision energy, and it has been revealed that an increase in collision energy first enhanced then decreased the degree of the product alignment and

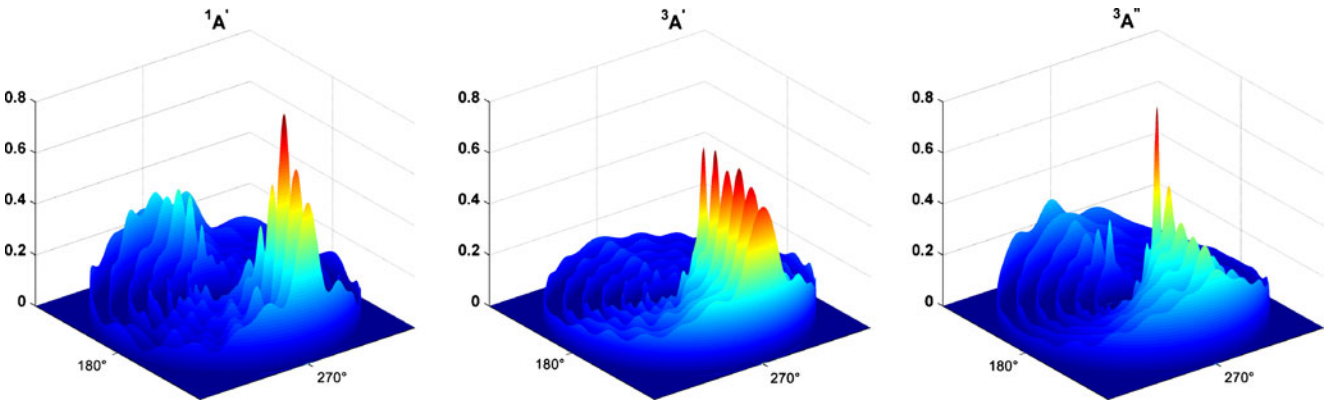

Fig. 6 The dihedral angle distributions of $P(\varphi_r)$ as a function of φ_r for F + HO → HF + O at the collision energies from 0.5 eV to 1.0 eV with an interval of 0.1 eV (from inside to outside)

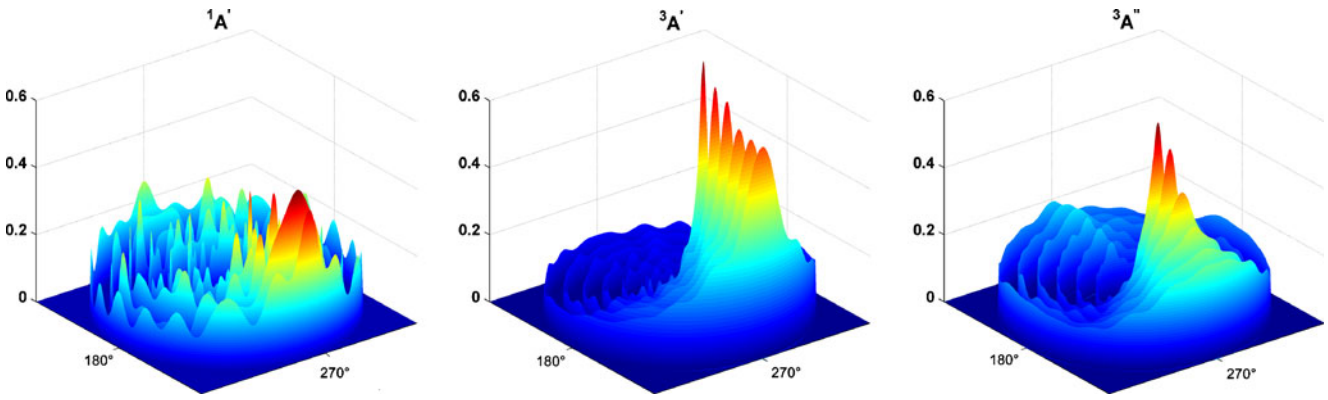

Fig. 7 The dihedral angle distributions of $P(\varphi_r)$ as a function of φ_r for F + DO → DF + O at the collision energies from 0.5 eV to 1.0 eV with an interval of 0.1 eV (from inside to outside)

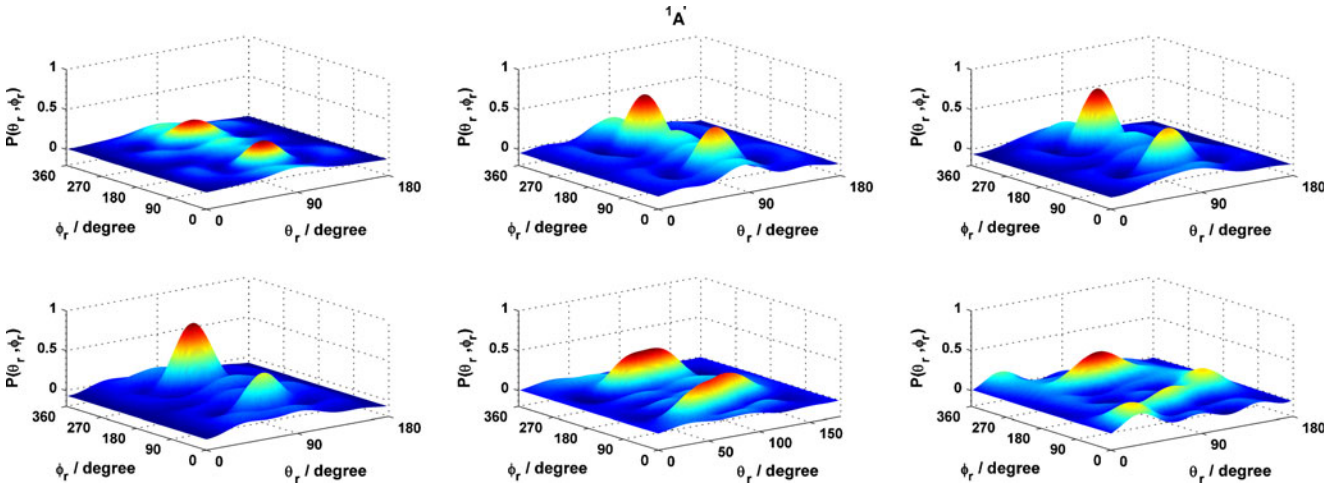

Fig. 8 Polar plots of $P(\theta_r, \varphi_r)$ distribution averaged over all scattering angles for F + HO on the ^{1}A' state for the collision energy from 0.5 to 1.0 eV (from left to right)

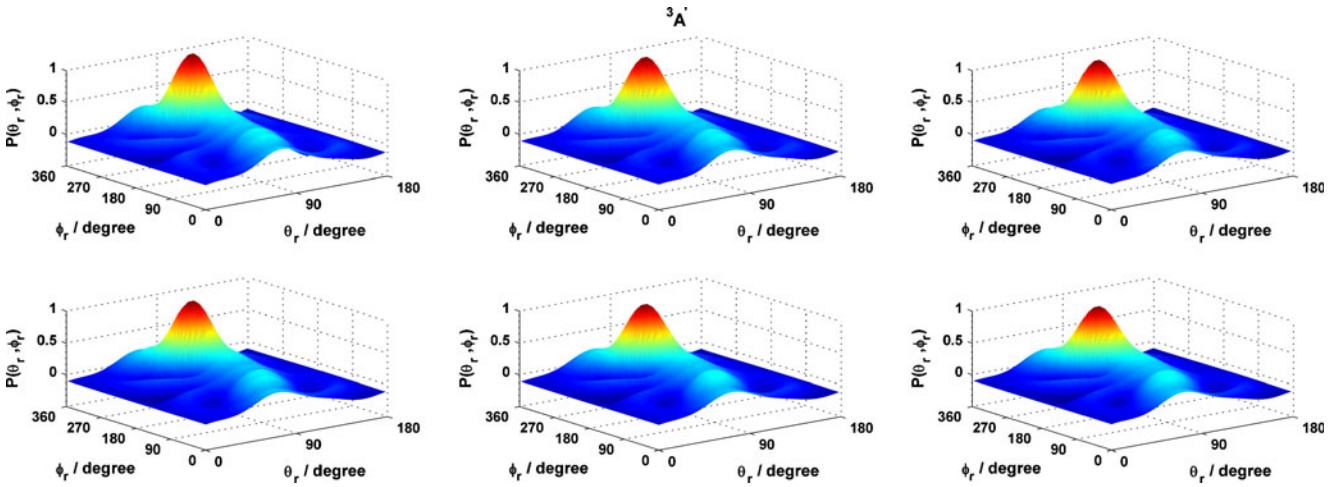

Fig. 9 Polar plots of $P(\theta_r, \varphi_r)$ distribution averaged over all scattering angles for F + HO on the ^{3}A' state for the collision energy from 0.5 to 1.0 eV (from left to right)

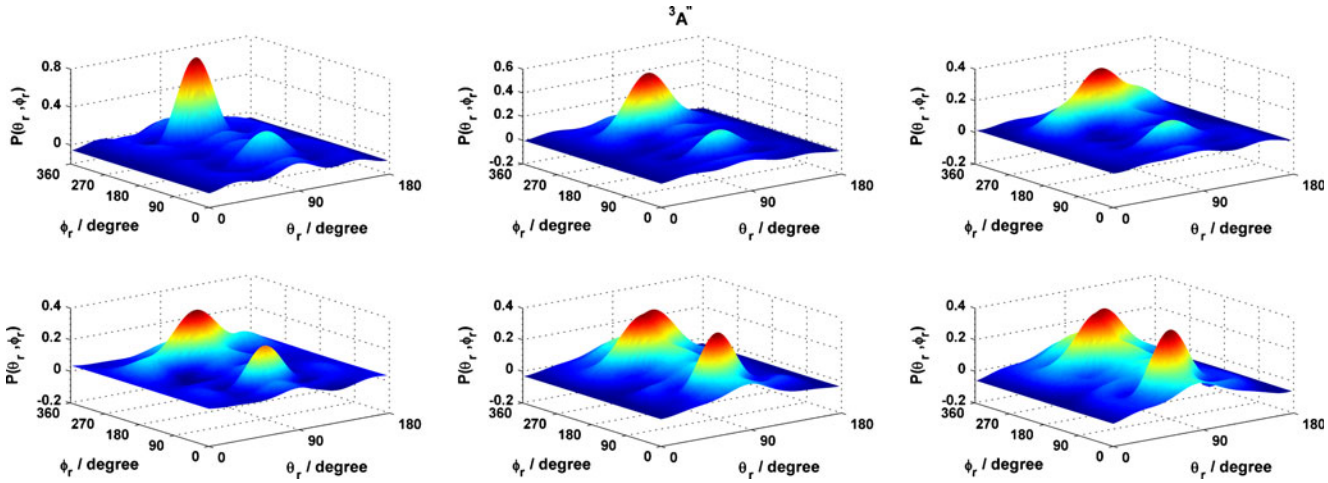

Fig. 10 Polar plots of $P(\theta_r, \varphi_r)$ distribution averaged over all scattering angles for F + HO on the ^{3}A" state for the collision energy from 0.5 to 1.0 eV (from left to right)

orientation on the singlet state but always weakened that on the two triplet states. Further, of the three electronic states, product polarization on the ^{3}A' state showed the least collision-energy-dependent behavior. On the other hand, there are pronounced isotope effects on all of the three electronic states, that is, product polarizations on the three states, especially on the singlet state, tend to become isotropic and thus be weakened with isotope substitution, also the trend with collision energy of the product polarization on the ^{3}A" state has been influenced remarkably by the isotope effect. The good agreement between the jointed $P(\theta_r, \varphi_r)$ distribution and the $P(\theta_r)$ and $P(\varphi_r)$ distributions in the reactive F + HO system, further confirmed and supported the present investigation about the chemical stereodynamics on the three electronic states. The different features of the potential energy surfaces of the three electronic states, in particular the existence of the deepest potential well on the singlet state and the relatively deeper hydrogen-bonded wells on the ^{3}A" state as well as the larger barrier height on the ^{3}A' state than on the ^{3}A" state, can explain the observed phenomena of the different product polarization behaviors on the three different electronic states.

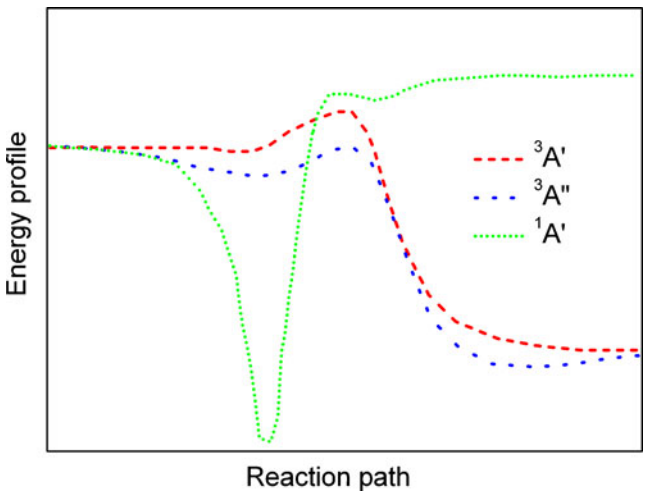

Fig. 11 Energy profiles along the minimum energy reaction path for the F + HO → HF + O reaction system

Acknowledgments This work was supported by National Science Foundation of China (10874096 and 20633070) and Qingdao University Foundation (063-06300510).

References

1. Sloan JJ, Watson DG, Williamson JM, Wright JS (1981) J Chem Phys 75:1190–1200
2. Walther CD, Wagner HG, Bunsenges B (1983) Phys Chem 87:403–409
3. Kornweitz H, Persky A (2000) Chem Phys Lett 331:132–136
4. Gomez-Carrasco S, Gonzalez-Sanchez L, Aguado A, Roncero O, Alvarino JM, Hernandez ML, Paniagua M (2004) J Chem Phys 121:4605–4618
5. Gomez-Carrasco S, Roncero O, Gonzalez-Sanchez L, Hernandez ML, Alvarino JM, Paniagua M, Aguado A (2005) J Chem Phys 123:114310
6. Gomez-Carrasco S, Hernandez ML, Alvarino JM (2007) Chem Phys Lett 435:188–193
7. Gomez-Carrasco S, Gonzalez-Sanchez L, Aguado A, Paniagua M, Roncero O, Hernandez ML, Alvarino JM (2004) Chem Phys Lett 383:25–30
8. Zhao J, Xu Y, Meng QT (2009) J Phys B-At Mol Opt Phys 42:165006
9. Zhao J, Xu Y, Yue DG, Meng QT (2009) Chem Phys Lett 471:160–162
10. Han BR, Zong FJ, Wang CL, Ma WY, Zhou JH (2010) Chem Phys 374:94–98
11. Zhao D, Zhang TY, Chu TS (2010) Can J Chem 88:893–897
12. Chu TS (2010) J Comput Chem 31:1385–1396
13. Blais NC, Truhlar DG (1977) J Chem Phys 67:1540–1546
14. Barnwell JD, Loeser JG, Herschbach DR (1983) J Phys Chem 87:2781–2786
15. Murray C, Orr-Ewing AJ (2004) Int Rev Phys Chem 23:435–482

16. Aquilanti V, Bartolomei M, Pirani F, Cappelletti D, Vecchiocattivi F, Shimizu Y, Kasai T (2005) Phys Chem Chem Phys 7:291–300
17. Wang ML, Han KL, He GZ (1998) J Phys Chem A 102:10204–10210
18. Wang ML, Han KL, He GZ (1998) J Chem Phys 109:5446–5454
19. Wang ML, Han KL, Zhan JP, Wu VWK, He GZ, Lou NQ (1997) Chem Phys Lett 278:307–312
20. Han KL, He GZ, Lou NQ (1996) J Chem Phys 105:8699–8704
21. Han KL, Zhang L, Xu DL, He GZ, Lou NQ (2001) J Phys Chem A 105:2956–2960
22. Zhan JP, Yang HP, Han KL, Deng WQ, He GZ, Lou NQ (1997) J Phys Chem A 101:7486–7489
23. Li RJ, Han KL, Li FE, Lu RC, He GZ, Lou NQ (1994) Chem Phys Lett 220:281–288
24. Wang ML, Han KL, Cong SL, He GZ, Lou NQ (1998) Chem Phys 238:481–485
25. Wang ML, Han KL, Zhan JP, Huang JH, He GZ (1998) Chem Phys 236:387–392
26. Zhan JP, Yang HP, Han KL, Wang ML, Deng WQ, He GZ, Lou NQ (1998) J Chem Phys 109:1819–1823
27. Zhang L, Chen MD, Wang ML, Han KL (2000) J Chem Phys 112:3710–3716
28. Li XH, Wang MS, Pino I, Yang CL, Ma LZ (2009) Chem Phys Phys Chem 11:10438–10445
29. Brouard M, Lambert HM, Rayner SP, Simons JP (1996) Mol Phys 89:403–423
30. Han KL, Zheng XG, Sun BF, He GZ, Zhang RQ (1991) Chem Phys Lett 181:474–478
31. Ju LP, Han KL, Zhang JZH (2009) J Comput Chem 30:305–316
32. Shaferray NE, Orrewing AJ, Zare RN (1995) J Phys Chem 99:7591–7603
33. Aoiz FJ, Brouard M, Enriquez PA (1996) J Chem Phys 105:4964–4982
34. Zhang X, Han KL (2006) Int J Quantum Chem 106:1815–1819
35. Greene CH, Zare RN (1983) J Chem Phys 78:6741–6753